NeuroImage 325 (2026) 121657

Contents lists available at ScienceDirect

NeuroImage

journal homepage: www.elsevier.com/locate/ynimg

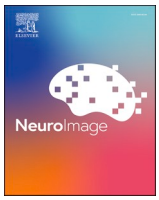

# Brain dynamic organization at the acute stage of severe brain injury

Gabriel Della Bella [a,b], Benjamine Sarton [c,d], Giulia Maria Mattia [d], Patrice Peran [d], Walter Lamberti [b], Pablo Barttfeld [a,1], Stein Silva [c,d,*]

[a] Cognitive Science Group. Instituto de Investigaciones Psicológicas (IIPsi, CONICET-UNC), Facultad de Psicología, Universidad Nacional de Córdoba, Córdoba, Argentina
[b] Facultad de Matemática Astronomía y Física (FaMAF), Universidad Nacional de Córdoba. Córdoba, Argentina
[c] Critical Care Unit. University Teaching Hospital of Purpan, Place du Dr Baylac, F-31059 Toulouse Cedex 9, France
[d] Univ Toulouse, Inserm, ToNIC, Toulouse, France

ARTICLE INFO

*Keywords:*
Brain injury
Disorders of consciousness
Brain states
Entropy
Mesocircuit
Prognosis

ABSTRACT

Acute Disorders of consciousness (DoC) poses significant clinical challenges, including early and accurate prognostication of neurological outcomes. Current assessment tools are limited in their predictive power, leaving many patients in a "gray zone" of uncertainty. While acute DoC are traditionally associated with structural brain damage, emerging evidence suggests that they are primarily driven by a withdrawal of excitatory synaptic activity across key cortical and subcortical regions, which can be captured through the dynamic analysis of resting-state brain activity. This study investigates the temporal dynamics of brain connectivity, shortly after severe brain injury (average of 13.9 days from onset), hypothesizing that acute DoC is marked by a global reorganization of functional connectivity and a shift toward less informative brain states, with distinct patterns emerging based on the underlying injury mechanism. Using functional magnetic resonance imaging (fMRI), we identify six distinct brain states across severely brain injured patients and healthy controls. These states, when sorted by decreasing entropy, span a continuum from state 1, characterized by high entropy, widespread positive long-distance coordination, and high global connectivity, predominantly observed in healthy controls, to state 6, which exhibits low entropy and minimal functional connectivity, and is predominantly associated with acute DoC. We demonstrate that the probability of occurrence of the more complex brain state correlates with improved neurological recovery at 3 months, as assessed by the Coma Recovery Scale–Revised (CRS-R). Hence, we were able to train a classifier based on brain state dynamics that achieved an accuracy of 78.5% in predicting patients' recovery potential (AUC = 0.864). Overall, our findings suggest that dynamic brain connectivity, particularly the entropy of brain states, can be a reliable early predictor of recovery from acute DoC, bridging the divide between theoretical advances and bedside medical decision-making.

## 1. Introduction

Acute Disorders of consciousness (DoC) is commonly defined as an insult to the brain that results in immediate disruption of normal brain functioning, typically manifested as altered consciousness (Giacino et al., 2014). Acute DoC presents both major clinical challenges and unique opportunities for fundamental scientific discoveries about the nature of human consciousness (Edlow et al., 2021). Hence, an early and accurate prediction of neurological outcome stands as the cornerstone of the clinical management of these patients (Nolan et al., 2021; Maas et al., 2017). However, current predictors are only informative in a subset of acute DoC patients, leaving up to half of them in a 'gray zone' of prognostication (Sandroni et al., 2021; Moseby-Knappe et al., 2020). This unmet need in terms of neuroprognostication has been recently identified as a major world-wide public health issue (Schiff, 2024). Importantly, it has been argued that this dismal situation is at least in part due to an incomplete understanding of brain injury impact over functional connectomes supporting conscious processing (Edlow et al., 2020). According to a prevailing view, acquired DoC are the deleterious consequence of irreversible brain structural damage. However, a growing body of evidence, suggests that the common pathophysiological underpinning of acute DoC, regardless of its etiology, is a broad

* Corresponding author.
*E-mail addresses:* silvastein@me.com, silva.s@chu-toulouse.fr (S. Silva).
[1] These authors contributed equally to the manuscript.

https://doi.org/10.1016/j.neuroimage.2025.121657
Received 24 February 2025; Received in revised form 21 November 2025; Accepted 16 December 2025
Available online 18 December 2025

withdrawal of excitatory synaptic activity across key neocortical and subcortical brain structures ("mesocircuit model") (Fridman et al., 2014). Indeed, seminal studies based on spontaneous brain activity recording have provided converging evidence about a relationship between mesocircuit component's functional disconnection and potential of neurological recovery from acute DoC (Malagurski et al., 2019; Peran et al., 2020; Sarton et al., 2024; Silva et al., 2010; Silva et al., 2015). It is worth noting that the vast majority of these reports assumed steady spatial-temporal fMRI signal interaction during the functional MRI (fMRI) scan period and therefore might have missed key brain dynamics.

Indeed, it has been recently demonstrated that brain activity constantly fluctuates in a tightly correlated manner across distant brain regions forming hierarchically organized reproducible whole brain "states". Crucially, such dynamical properties have been proposed as reliable mechanistic signatures of consciousness (Barttfeld et al., 2015; Demertzi et al., 2019; Uhrig et al., 2018). Hence, experiments with fMRI across different sleep stages and during anesthesia, both in human (Demertzi et al., 2019) and animal (Barttfeld et al., 2015) models, have shown that the brain spontaneously generates a dynamic series of activity patterns that evolve over time. In the specific setting of DoC, available evidence collected months to years after severe brain injury, suggest that fully unresponsive patients in vegetative state/ unresponsive wakefulness syndrome (VS/UWS) have smaller span of dynamic brain states than those in minimally conscious state (MCS) (Demertzi et al., 2019). Nevertheless, despite the promise held by the investigation of the dynamic repertoire of resting state brain activity early after brain injury, currently, the specific alterations in brain dynamics associated with acute DoC remains unknown.

Based on current neuronal theories of consciousness (Storm et al., 2024) which suggest that the pattern of neuronal interactions that are relevant for consciousness must be differentiated and information rich (Dehaene and Changeux, 2011), we sought to investigate the temporal dynamic of ongoing brain activity and its coordination over distant cortical regions at the early phase of acute DoC. We postulate that acute DoC are associated with the global reorganization of brain functional connectivity, implicating mesocircuit regions and causing a shift of brain states towards less informative functional configurations. Moreover, we hypothesize that the primary brain injury mechanisms responsible for acute DoC have specific functional fingerprints that can be detected early after brain injury onset. Finally, we also expect that there is a relationship between the dynamic functional repertoire identified at the acute DoC and the patient's neurological outcome at 3 months.

## 2. Methods

### 2.1. Experimental design

Cross-sectional study of traumatic and anoxic patients with acute DoC and compared with matched controls from one previous prospectively collected dataset [COMA-3D (NCT 01,620,957)] (Sarton et al., 2024; Mattia et al., 2022). This former prospective study aimed to investigate the predictive value of MRI and in vivo molecular imaging in acute DoC and was undertaken in three intensive care units affiliated with the University Hospital of Toulouse (Toulouse, France) between February 2018 and February 2022. Clinical assessment and demographic data collection (Glasgow Coma Scale, GCS; Full Outline of Unresponsiveness, FOUR) (Ahmadi et al., 2023; Wijdicks et al., 2005) were performed at baseline by certified assessors (SS and BS) and patients were followed up at 3 months after primary brain injury using the revised version of the Coma Recovery Scale (CRS-R) (Schnakers et al., 2008) (Table 1). MRI data were collected shortly after injury (mean time = 14 days, range = 2–34 days) and in all the cases, at least 2 days (4 ± 2 days) after complete withdrawal of sedation and under normothermic conditions. The study was approved by the Ethics Committee of the University Teaching Hospital of Toulouse, France. In all instances, informed and written consent to participate in the study was obtained from the subjects themselves in the case of healthy subjects and from legal surrogates of the patients. In case the patient recovered sufficient capacity for discernment during the trial, she/he was informed that the

**Table 1**
**Patient's demographic and clinical data.** Abbreviations. BI= Brain injury; BS= Brainstem; CC=Corpus callosum; DAI= Diffuse axonal injury; CRS-*R*= Coma Recovery Scale Revised at 3 month; DGN: Depp grey nucleus; *F*=female; FOUR (Full Outline of UnResponsiveness (*E* = Eye; *M* = Motor; *B* = Brainstem; *R* = Respiration) Fr=Frontal; GCS= Glasgow coma scale (*E*=Eye; *V*=Verbal; *M*=Motor); *M*=Male; MCS: minimally conscious state; Occ= Occipital cortex; Pc=Parietal cortex; SAH= Sub arachnoid hematoma; SDH= Subdural hematoma; UWS=unresponsive wakefulness syndrome. [1] Myoclonic status epilepticus; best GCS before dying = 3; [2] WLST 13 says post-ICU admission; best GCS before dying = 6; [3] WLST 1-month post-ICU admission; best GCS before dying = 3; [4] Death at 2-month post- ICU discharge of respiratory failure. Best neurological state before dying: unresponsive wakefulness syndrome (CRS-*R* = 5).

| Patient | Age | Sex | BI | GCS | FOUR | 3 months CRS-R | Standard brain MRI findings |
|---|---|---|---|---|---|---|---|
| P.1 | 18 | F | Anoxic | 6(E1V1M4) | 5 (E0M2B3R0) | UWS / 3 | DGN, CC. FLAIR hyperintensity |
| P.2 | 65 | F | Anoxic | 9(E4V1M4) | 8 (E3M2B2R1) | MCS /17 | Striatal, Occ. FLAIR hyperintensity |
| P.3 | 59 | M | Anoxic | 5(E1V1M3) | 3 (E0M1B2R0) | UWS /5 | Striatal, Occ. FLAIR hyperintensity |
| P.4 | 59 | M | Anoxic | 3(E1V1M1) | 1 (E0M0B1R0) | Death[1] | Striatal FLAIR hyperintensity |
| P.5 | 30 | F | Anoxic | 4(E1V1M2) | 4 (E0M1B3R0) | UWS /4 | Striatal Pc. /Occ. FLAIR hyperintensity |
| P.6 | 23 | M | Anoxic | 6(E1V1M4) | 8 (E0M3B4R1) | EMCS /21 | Normal |
| P.7 | 55 | M | Anoxic | 4(E2V1M1) | 2 (E1M0B1R0) | UWS /3 | Cortical occipital FLAIR hyperintensity |
| P.8 | 67 | F | Anoxic | 5 (E2V1M2) | 3 (E1M1B1R0) | Death[2] | Normal |
| P.9 | 59 | M | Anoxic | 3(E1V1M1) | 0 (E0M0B0R0) | Death[3] | Occipital cortical T1 hyperintensity |
| P.10 | 45 | M | Anoxic | 9(E4V1M4) | 10 (E2M3B4R1) | MCS /17 | Normal |
| P.11 | 52 | M | Anoxic | 3(E1V1M1) | 0 (E0M0B0R0) | UWS /3 | CC and Pc-Occ FLAIR hyperintensities |
| P.12 | 39 | F | TBI | 4(E1V1M2) | 5 (E0M2B3R0) | UWS /7 | Thalamic petechiae; DAI; SAH |
| P.13 | 23 | M | TBI | 7(E1V1M5) | 4 (E0M3B3R1) | EMCS /23 | Hemispheric contusion; Fr. petechiae; SAH |
| P.14 | 21 | F | TBI | 5(E1V1M3) | 6 (E0M2B4R0) | EMCS /23 | CC contusion; DAI; SAH |
| P.15 | 36 | M | TBI | 8(E2V1M5) | 7 (E1M3B2R1) | EMCS /23 | Fr. / CC. contusion; SAH |
| P.16 | 40 | M | TBI | 3(E1V1M1) | 0 (E0M0B0R0) | EMCS /23 | Fr. petechiae; SDH; SAH |
| P.17 | 70 | M | TBI | 5(E1V1M3) | 4 (E0M2B2R0) | MCS /17 | Temporal contusion; SDH; DAI; SAH |
| P.18 | 79 | M | TBI | 8(E3V1M4) | 8 (E1M3B3R1) | Death[4] | Fr petechiae; DAI; SDH; SAH |
| P.19 | 22 | F | TBI | 8(E4V1M4) | 7 (E2M3B1R1) | EMCS /23 | DAI (corpus callosum, frontal); SAH |
| P.20 | 32 | M | TBI | 8(E3V1M4) | 7 (E1M3B3R0) | UWS /9 | DAI; Interpeduncular SAH |
| P.21 | 69 | M | TBI | 6(E1V1M4) | 6 (E0M3B3R1) | UWS /4 | DAI |
| P.22 | 21 | M | TBI | 7(E2V1M4) | 8 (E0M3B4R1) | EMCS /23 | CC- DAI, SDH |
| P.23 | 19 | F | TBI | 9(E4V1M4) | 10 (E3M3B3R1) | MCS /17 | DAI, CC and left mesencephalic contusion |
| P.24 | 57 | M | TBI | 6(E1V1M4) | 4 (E0M3B1R0) | UWS /2 | DAI; mesencephalic/BS hyperintensities |
| P.25 | 20 | F | TBI | 7(E2V1M4) | 5 (E1M3B1R1) | MCS /12 | DAI |

study was or has been performed, and consent was obtained from her/him.

### 2.2. Participants

The patient group consisted of 25 patients (16 males; mean age = 43.2 years; range = 18–79 years) that were included in the study after they had a behavioral assessment with GCS and had been diagnosed as being acute DoC injury (GCS score at the admission to the hospital $\leq 9$ with motor responses $< 6$) induced by either traumatic or anoxic mechanisms (Table 1 and Table S1). Patients needed to maintain a GCS score $\leq 9$ with motor response $< 6$ without sedation at the time of brain imaging acquisition. All patients exhibited only reflex (e.g. non-intentional) behaviors, including the complete absence of visual pursuit, at the time of MRI scanning. Patients not meeting this criterion at assessment were excluded. Additional exclusion criteria were significant neurological or psychiatric illness prior to acute brain injury. All patients were managed according to standard of care recommendations by physicians blinded to neuroimaging data. To avoid confounding factors, all patient assessments were conducted at least 2 days ($4 \pm 2$ days) after complete withdrawal of all sedative drug therapy and were performed under normothermic conditions. On the day of brain imaging, urine benzodiazepine and barbiturate screening tests were used in patients to rule out residual sedation in cases of prolonged utilization of these drugs. Over the same recruitment period, 23 controls, matched by age and sex, were recruited (15 males; mean age = 44 years; range = 20–75 years). The control subjects had no history of neurological or psychiatric disorders and were included only if they presented a normal neurological examination result.

### 2.3. Clinical assessment

In patients, standardized clinical examination was performed by certified raters blinded to neuroimaging data on the day of the patient's admission to the hospital and the day of MRI scanning. The patient's neurological outcome was assessed 3 months after the primary brain injury by using the CRS-R. The CRS-R is a 23-point scale measuring arousal level, auditory, language, visual-perception, communication abilities and motor function. This scale enables the distinction between patients in VS/UWS and patients in a MCS or patients who emerged from MCS (EMCS) and recovered consciousness as reflected by functional communication or functional use of objects. According to this scale, the patient's 90 days outcome was binarized as either favorable (MCS or EMCS) or unfavorable (VS/UWS or deceased).

### 2.4. Imaging acquisition and preprocessing

The fMRI data was acquired in a 3T (Intera Achieva; Philips, Best, The Netherlands) scanner (TR = 1.3 s; TE = 30 ms, FOV = 240 mm), consisting of one session of 500 scans or 650 s. A T1 image was also collected (TR = 8.1 ms, TE = 3.7 ms, FOV = 220–232–170 mm, flip angle = 8°, resolution = 1 mm3 isovoxel). Monitoring of vital measures was performed by a senior intensivist throughout the experiment.

Preprocessing was conducted using the CONN toolbox (RRID: SCR_009550) version 21.a running in MATLAB 2016a. Standard preprocessing steps were applied: realignment and unwarping, slice timing correction, co-registration to the structural image, segmentation, normalization to MNI space and a 8 mm FWHM smoothing (Peran et al., 2020; Mattia et al., 2022). We regressed out nuisance signals of white matter, cerebrospinal fluid, and realignment parameters by means of the anatomical component-based noise correction algorithm (aCompCor). Then, we applied a band-pass filter at 0.008–0.09 Hz. The BOLD time series of each voxel was averaged over the Regions of Interest (ROIs) defined by the Willard 499 atlas (Richiardi et al., 2015). We decided to focus our analyses in the Default Mode Network (DMN), given its established relevance in disorders of consciousness (Boly et al., 2007; Vanhaudenhuyse et al., 2010; Boly et al., 2012). To isolate the ROIs associated with the DMN, we cross-referenced the Willard Atlas with the AAL template. This process allowed us to identify and label the specific regions within the DMN and ultimately, a subset of 34 ROIs was used for further analysis. Aiming to investigate the putative implication of mesocircuit, regions of interest (ROIs) belonging to this empirical model were defined and further subdivided. First, we subdivided the DMN into its dorsal and ventral components, then we studied the connectivity of four specific groups of ROIs (subnetworks): Thalamus, Posterior Cingulate Cortex (PCC), Anterior Cingulate Cortex (ACC) and Medial Prefrontal Cortex (mPFC) (Fig. S1 and Supplementary Material).

### 2.5. Dynamic functional connectivity analysis

To capture the dynamic functional connectivity, a sliding window approach was implemented with a window size of 30 scans (39 s), shifted by 16 scans (20.8 s), resulting in a total of 30 windows per subject. These parameters were chosen to replicate previously reported time windows (Barttfeld et al., 2015; Allen et al., 2014; Demertzi et al., 2015). The dynamic functional connectivity was estimated by using the Pearson correlation between all pairs of ROIs in the DMN which results in matrices of size $34 \times 34$. In order to obtain the recurring patterns of connectivity we used an unsupervised k-means clustering algorithm, a method that was previously used in fMRI (Allen et al., 2014; Demertzi et al., 2015) and EEG (Michel and Koenig, 2018). This algorithm was applied to a dataset that combined both controls and patients, allowing the identification of a common state space shared across all participants. In this framework, the clustering was not used to assign individuals to a specific group but to define a set of recurring connectivity patterns (brain states) that can be expressed by any subject, patient or control, with different probabilities of occurrence. This joint approach ensures that comparisons between groups are performed within the same functional space, enabling a direct assessment of how the temporal distribution of shared brain states differs between healthy and injured brains. To determine the optimal number of clusters (k), we applied the elbow method, plotting the within-cluster sum of squares against increasing values of k and selecting the point at which the curve showed a clear "elbow", in this case at $k = 6$, indicating a balance between model complexity and explained variance (Fig. S2b). The upper triangular part of the connectivity matrices, comprising 561 values, were used as input features. To mitigate the risk of convergence to a local minimum inherent to the k-means algorithm, we repeated the procedure 1000 times (also known as replicates) and retained the solution with the lowest total within-cluster sum of squares. Subsequently, each dynamic connectivity matrix was classified based on its proximity to the closest brain state by means of the euclidean distance. The probability of occurrence pi of brain state i was calculated by counting the number of times it appears divided by the total number of matrices. We also computed the dwell time, defined as the average time a subject is in a given brain state. We calculated the entropy of each brain state, denoted as Hi, by first extracting the connectivity values from the brain state matrix and vectorizing them into a one-dimensional array. We then estimated the distribution of these values by computing a histogram, using a number of bins determined by the square root rule (i.e., $\sqrt{561} \approx 24$, where 561 is the number of unique pairwise connections in a $34 \times 34$ matrix, excluding the diagonal and redundant entries). The entropy of the resulting distribution was computed using the Shannon entropy formula:

$$H_i = -\sum_{j=1}^{24} f_{ij} log\left(f_{ij}\right)$$

where $f_{ij}$ is the frequency of bin j in brain state i.

To summarize the distribution of brain states and corresponding entropy values of a given subject we introduced a Weighted Entropy measure defined as:

$$WE = \sum_{i=1}^{6} p_i \cdot H_i$$

where $p_i$ is the probability of state i and $H_i$ its entropy. We selected WE as our primary metric as it jointly captures the informational complexity of each brain state and its temporal prevalence, offering a compact representation of the brain's dynamic repertoire. Unlike traditional entropy measures applied to univariate time series (e.g., sample or permutation entropy), this approach operates on time-resolved connectivity matrices and reflects both spatial and temporal dimensions of brain organization. This analysis was applied to two different groups: one where we included both controls and patients and another where we only used the patients. This was done in order to focus specifically on the part of the multidimensional space occupied by patient data and to obtain a more detailed clustering analysis. To better characterize the brain states we calculated the mean connectivity of the ROIs in a sub-network (intra-connectivity) and between sub-networks (inter-connectivity) comparing connectivity matrices classified as State 1 and connectivity matrices classified as State 6 (Fig. 1). Intra-connectivity was defined as the average of all pairwise correlations between ROIs belonging to the same subnetwork (e.g., all ROIs within the thalamus, PCC, ACC, or mPFC). Inter-connectivity was defined as the average of all correlations between ROIs belonging to different subnetworks (e.g., thalamus–ACC, PCC–mPFC, etc.). These values were used to quantify the internal coherence of each subnetwork and the degree of functional coupling between subnetworks across the identified brain states. To further characterize the relationships among the identified connectivity states, we computed a dendrogram using Euclidean distances between the centroid matrices and Ward's linkage criterion (Supplementary Fig. S2c). We also included in the same figure the distribution of cluster occurrences across patients and controls (Supplementary Fig. S2d).

### 2.6. Connectivity of subnetworks

In the present study, embedded in the anterior forebrain mesocircuit theoretical framework, we focused on large-scale cortical networks, to maintain consistency with previous literature and ensure interpretability of the dynamic connectivity measures. In order to study the connectivity of the DMN we subdivided it into two components: dorsal (DMNd) and ventral (DMNv; Fig. S1 and Supplementary Material) (Andrews-Hanna et al., 2010). Although our primary analyses were focused on the DMN, for consistency and interpretability, we also performed a supplementary whole-brain control analysis using the complete Willard atlas. As shown in Supplementary Fig. 6 the main findings, including the group differences between patients and controls and the prognostic value of brain-state dynamics, were preserved when considering the entire brain, confirming the robustness and generality of the results. The within-network was calculated by averaging all ROIs from each network and the between-network connectivity by averaging the connectivity between ROIs from the dorsal and ventral subnetworks in matrices that were classified as State 1 and State 6 which represent the highest and lowest entropy states, respectively. We selected these two extreme states, rather than including all intermediate states, in order to simplify the analysis and highlight the maximal contrast in connectivity dynamics across the entropy spectrum. Then we looked at four specific ROIs: Thalamus, PCC, ACC and mPFC and repeated a similar procedure, but instead of the within-network connectivity we calculated the connectivity between the ROI and the rest of the brain. This is because the Thalamus was composed of a single ROI which makes calculating the intra-network not possible

### 2.7. Relationship with patient's outcome

We performed a comprehensive analysis to assess the predictive capacity of brain states for patient outcomes, using both weighted entropy and the probability of brain states as metrics. Following a three-period post–brain injury, patients underwent assessment using the CRS-R. We assigned a binary outcome of 0 when the patient either deceased or remained in VS/UWS at the end of the follow-up period, and 1 when the patient evolved to MCS or EMCS. This binary variable served as the target in the predictive analysis.

To evaluate the predictive power of weighted entropy (WE), we conducted a leave-one-out cross-validation analysis (Fig. 1). For each iteration, all patients except one were used to define the brain state clusters, ensuring that the subject left out did not contribute in any way to the estimation of the model, thus avoiding data leakage and biased performance. Because age differed significantly between the favorable and unfavorable outcome groups, we incorporated an age-stratified resampling procedure within each leave-one-out iteration to reduce potential confounding. Specifically, after removing the test subject, the remaining training set was divided into four age bins (18–35, 35–50, 50–65, 65–100 years). We computed the proportion of patients within each bin and generated a stratified training set by sampling within each age bin (with replacement when necessary) according to these proportions. This ensured that each training set preserved the original age distribution while preventing systematic biases arising from the fact that subjects with better outcomes tended to be younger.

To quantify uncertainty in these performance metrics, we applied a jackknife resampling procedure, in which, for each leave-one-out iteration, the metric was recomputed with the corresponding observation removed. From the resulting set of jackknife estimates, we computed the mean and standard error for accuracy, precision, recall, F1-score, and AUC following standard jackknife formulas.

In order to compare demographic and clinical characteristics between the two outcome groups we ran a two-sample independent *t*-test to assess differences in age, GCS and follow-up CRS-R, as well as a Chi-squared test to assess differences between etiology and sex. A partial correlation was conducted to examine the association between WE and binary outcome, controlling for age, sex, GCS, and etiology.

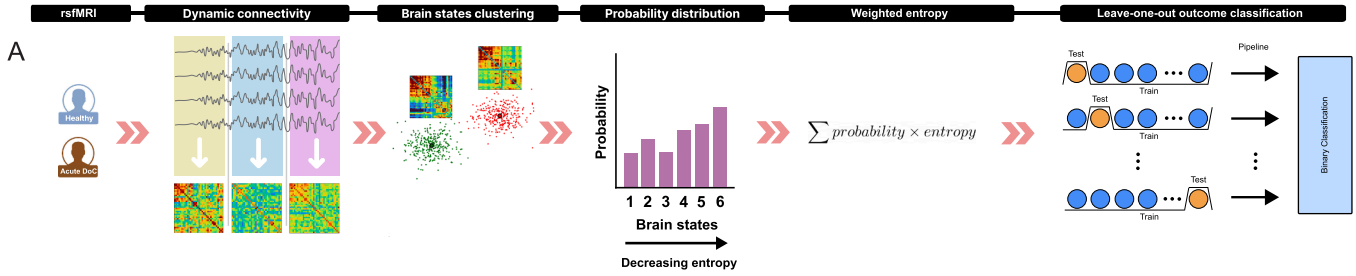


**Fig. 1. Analysis pipeline.** A) We utilized an fMRI dataset consisting of 23 controls and 25 patients with acute DoC. Windowed correlation matrices were computed, followed by clustering analysis to identify two distinct brain states. The probability of occurrence of these brain states was compared between controls and patients, as well as between patients with favorable and unfavorable outcomes. Finally, we applied a leave-one-out approach to evaluate the potential of this analysis for prognosis.

### 2.8. Statistical analysis

In order to quantify the differences between groups we used a linear regression model implemented using the Python library Statsmodels version 0.14.0 (Supplementary Material). To examine the relationship between the subject's group and the probability of a brain state (as well as for the dwell time), we considered both group membership and demographic factors such as age and sex as covariates. The model incorporated a categorical variable for group (Control vs. Patient) and sex (Female vs. Male) as well as age to account for potential confounding variables. For the analysis of brain state differences across sub-networks, we used separate models for each sub-network, including both intra- and inter-network connections. These values were corrected for multiple comparisons using False Discovery Rate (FDR) at a 5 % significance level. Each model incorporated brain state (State 1 or State 6), as well as age and sex, as explanatory variables to control for individual differences in connectivity measures. In order to evaluate the statistical significance of our classifier we used Fisher's exact test which is more suitable for small sample sizes than the classical $\chi^2$ test. This test is used to compare the contingency table of the classifier against one obtained by random chance.

## 3. Results

### 3.1. Dynamic brain states at the early phase of severe brain injury

Our analysis modeled brain activity using six recurrent brain states, as defined by K-means clustering with $k = 6$ (Fig. 2a and S2a). These states form a continuum, ranging from highly integrated to globally disconnected network configurations. State 1, which exhibited the highest entropy (Entropy = 4.34), was characterized by predominantly positive correlations within the ventral and dorsal DMN, as well as strong positive connectivity between the two subnetworks. In contrast, State 6, which had the lowest entropy (Entropy = 4.05), showed markedly weaker correlations within both the ventral and dorsal DMN. The intermediate states progressively transitioned between these two extremes, reflecting a gradual loss of integration and complexity in DMN connectivity. We also computed the dwell time for controls and patients, that is, the average time each subject is in a given brain state (Fig. S3), but found no statistically significant difference between groups ($\beta = 0.13$, SE = 0.07, $p = 0.08$). Looking at the connectivity matrices that were classified as State 1 and State 6 and averaging the values within sub-networks reveal consistently higher correlation values in State 1 vs. State 6 in the dorsal and ventral DMN (Fig. 2b, left) (Dorsal: $\beta = -0.19$, SE = 0.01, $p = 4 \times 10^{-27}$, Ventral: $\beta = -0.03$, SE = 0.01, $p = 0.04$) as well as in the connectivity between them (Fig. 2b, right) (Dorsal-Ventral: $\beta = -0.07$, SE = 0.02, $p = 0.0001$). When looking at the connectivity within and between the selected ROIs, we found the mean connectivity

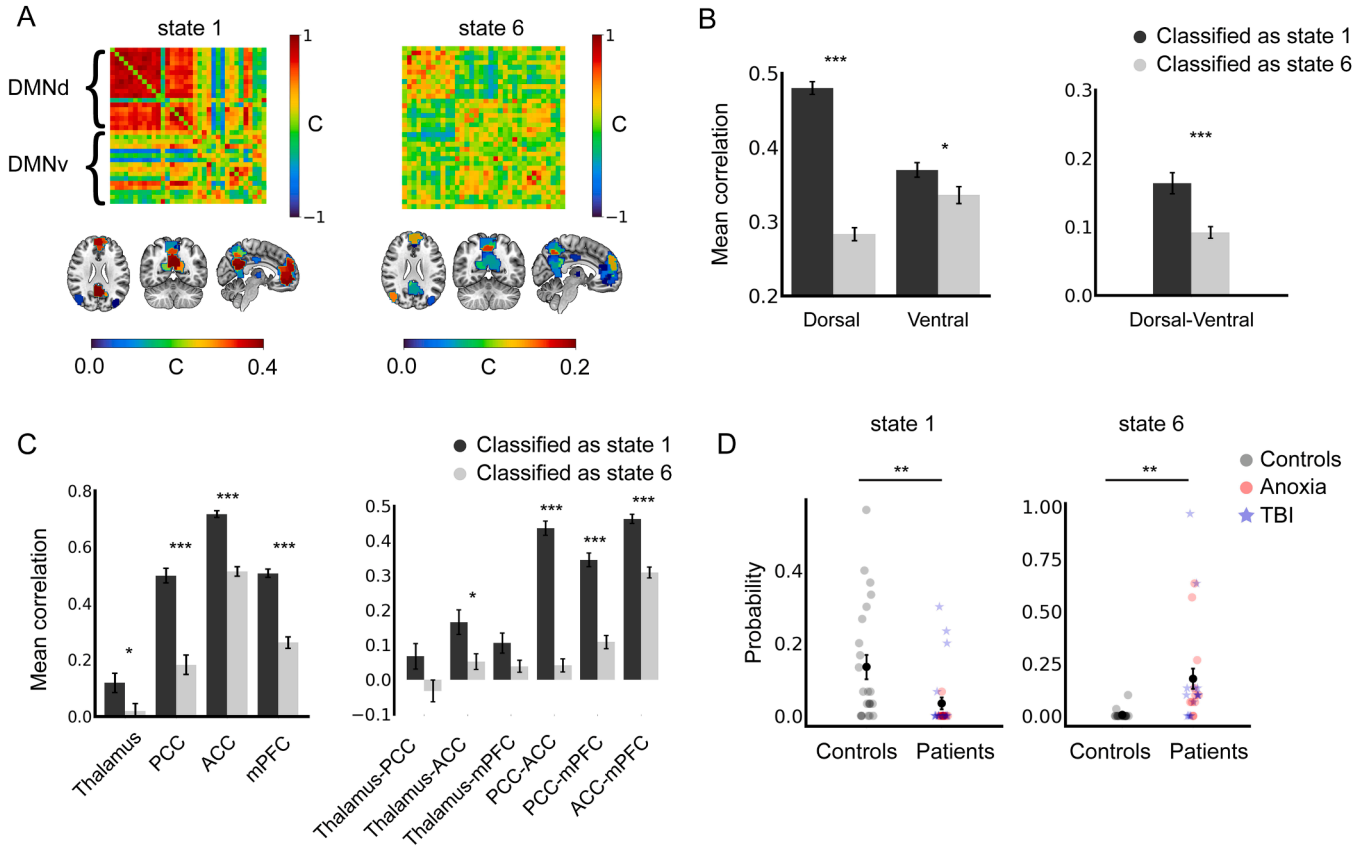


**Fig. 2. Brain states and their relation to clinical conditions.** A) Brain states obtained from the clustering analysis. These two brain states have different connectivity patterns: State 1 consists mostly of positive correlation values, particularly in the DMNd, (dorsal DMN). State 6, on the other hand, consists of lower correlation values, specifically in the DMNd compared to State 1, and in the correlation between DMNd and DMNv (ventral DMN). B) Mean correlation in Dorsal and Ventral DMN. The dynamic connectivity matrices that were classified as State 1 presented a higher mean connectivity value than those classified as State 6 consistent across the two sub-networks. C) Mean correlation in Thalamus, PCC, ACC and mPFC sub-networks. The dynamic connectivity matrices that were classified as State 1 presented a higher mean connectivity value than those classified as State 6. This was consistent across sub-networks both in intra and inter connectivity. D) Probability distribution of brain states. State 1 is predominantly present in controls and less present in patients, and the reverse is true for State 6. $*p < 0.05$, $**p < 0.01$, $***p < 0.001$. All p-values were corrected for multiple comparisons using FDR at a 5 % significance level.

to be consistently higher in connectivity matrices classified as State 1 compared to those classified as State 6 when comparing the ROI with the rest of the brain (Fig. 2c, left) (Thalamus: $\beta = -0.10$, SE = 0.04, $p = 0.03$; PCC: $\beta = -0.31$, SE = 0.04, $p = 1 \times 10^{-9}$ ACC: $\beta = -0.20$, SE = 0.02, $p = 4 \times 10^{-14}$ mPFC: $\beta = -0.24$, SE = 0.02, $p = 4 \times 10^{-14}$) as well as when comparing ROIs between them (Fig. 2c, right) (Thalamus-ACC: $\beta = -0.11$, SE = 0.04, $p = 0.01$; PCC-ACC: $\beta = -0.39$, SE = 0.03, $p = 3 \times 10^{-22}$; PCC-mPFC: $\beta = -0.23$, SE = 0.03, $p = 4 \times 10^{-12}$; ACC-mPFC: $\beta = -0.15$, SE = 0.02, $p = 4 \times 10^{-10}$). All p-values were corrected for multiple comparisons using FDR at a 5 % significance level.

### 3.2. Fingerprints of consciousness abolition

Fig. 2d illustrates the distribution of brain states across controls and patients with acute DoC. State 1 was mostly associated with the awake state of the controls and was less present in patients, while the opposite was observed in State 6. Significant differences were observed in Controls vs. Patients, using a linear regression model (see Methods) with Group (Control or Patient), Age and Sex as predictors and the probability of a brain state as a target. The probability of State 1 was significantly reduced in patients compared to controls (group, $\beta = -0.10$, SE = 0.03, $p = 0.005$; sex, $\beta = -0.01$, SE = 0.04, $p = 0.64$; age, $\beta = -0.0021$, SE = 0.001, $p = 0.03$). The likelihood of each brain state (Fig. 2d) was consistently influenced by the subject's condition. These results are in line with prior studies indicating that high entropy states are linked to conscious processing (Barttfeld et al., 2015; Allen et al., 2014; Demertzi et al., 2015). Although the probability of State 2, 3, 4, and 5 show a trend in the expected direction (State 2 with high entropy is more frequent in controls and State 5 with low entropy is more frequent in patients) it did not show a statistically significant difference in these states.

### 3.3. Neuroprognostication value

To assess the prognostic utility of brain state dynamics, we implemented a leave-one-out cross-validation approach using Weighted Entropy (WE) as the predictive feature. For each iteration, one patient was excluded, and the WE distribution was modeled based on the remaining patients, stratified by clinical outcome. The excluded patient's outcome was then predicted by comparing their WE value to these distributions. This approach yielded robust classification performance, with a statistically significant association between predicted and actual outcomes as determined by Fisher's exact test ($\chi^2 = 30.0$, $p = 0.003$). The model achieved an accuracy of 82.6 ± 1.7 %, with an area under the ROC curve (AUC) of 0.835 ± 0.017, a precision of 75.0 ± 2.8 %, a recall of 90.0 ± 2.1 % and an F1-score of 81.8 ± 1.9 % (Fig. 3). Notably, the classifier correctly identified 9 out of 12 patients with favorable outcomes (75.0 %) and 10 out of 11 patients with unfavorable outcomes (90.9 %), demonstrating a high sensitivity for detecting potential recovery and clinically meaningful discrimination at the individual level.

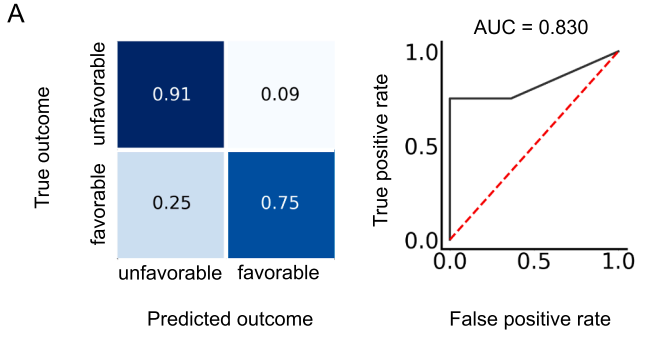


**Fig. 3. Brain states and their relation to patients' prognosis.** Binary classification of outcome. The confusion matrix reveals a classification with high sensitivity (75.0 %) and high specificity (90.9 %) as well as a ROC with AUC = 0.830.

Baseline demographic and clinical variables, except for age, did not significantly differ between patients with favorable and unfavorable outcomes. In particular, initial GCS (t (Schnakers et al., 2008) = 1.27, $p = 0.22$), etiology ($\chi^2$ (Giacino et al., 2014; Boly et al., 2007) = 2.09, $p = 0.15$), sex ($\chi^2$ (Giacino et al., 2014; Boly et al., 2007) = 0.08, $p = 0.77$) did not differ significantly between groups. However, we did find a significant difference in age (t (Schnakers et al., 2008) = 2.65, $p = 0.02$). A partial correlation was conducted to examine the relationship between WE and binary outcome, controlling for age, sex, GCS, and primary brain injury mechanism. The association was not statistically significant (r-partial (Schnakers et al., 2008) = −0.24, 95 % CI [−0.62, 0.24], $p = 0.33$). To provide a clinical characterization of the observed brain-state variability, we divided patients according to the median of their Weighted Entropy (high vs. low WE) and compared age and initial GCS as baseline measures. No significant differences were found between groups, indicating that the variability in brain-state dynamics is not explained by demographic or clinical severity factors (Supplementary Fig. S4). This analysis rules out the possibility that the observed prognostic effects of brain-state dynamics are driven by baseline demographic or clinical differences between groups.

## 4. Discussion

We investigated the brain's dynamic organization during acute DoC, with the aim of determining very early patterns of spontaneous signal coordination specifically associated with consciousness abolition, primary brain injury and patient's potential of recovery. We identified six distinct brain states characterized by recurrent patterns of dynamic functional connectivity. Among the six identified brain states, two exhibited the most pronounced contrast in both network organization and frequency of occurrence. One state—predominantly observed in healthy controls— (State 1) was characterized by robust long-range positive correlations within and between the dorsal and ventral components of the default mode network (DMN), as well as high overall entropy. This configuration reflects a rich and flexible dynamic repertoire, compatible with preserved thalamo-cortical communication and high integrative capacity. These features are in line with information-theoretic accounts of consciousness and prior evidence linking high-entropy brain configurations with conscious processing (Mateos et al., 2016; Mateos et al., 2018; Carhart-Harris et al., 2014).

In contrast, the state most frequently observed in patients with acute DoC (State 6) exhibited markedly diminished functional connectivity, particularly within key DMN regions such as the thalamus, anterior and posterior cingulate cortices, and medial prefrontal cortex. This state also showed the lowest entropy values, indicating a restricted repertoire of functional configurations and a shift toward rigid dynamics. These alterations are consistent with large-scale network fragmentation and support the hypothesis that structural and metabolic disruptions within the DMN contribute critically to impaired consciousness.

Regarding the dynamic functional reconfiguration that was observed in brain injured patients, it is worth noting that we have identified a significant shift from positive toward negative long-distance signal coordination. This observation is in line with the prediction of the Global Neuronal Workspace theory stating that different streams of information in the brain compete for global information dissemination (Baars, 2005). In terms of the spontaneous fMRI signal, this could manifest in the mutual inhibition of activity at different cortical regions, which can be unbalanced by brain injury, ultimately leading to overriding anti-correlated dynamics.

Finding timely and reliable predictors of neurological outcome from DoC represents an outstanding open problem for science. Regardless of primary brain injury mechanisms, we have provided multiple and converging lines of evidence about the potential use of brain dynamics assessment for early neuroprognostication. To further characterize the link between brain dynamic organization and patient's neurological

outcome, we applied a leave-one-out classification where each patient's outcome was classified based on the entropy of the rest of the patients. The classifier correctly categorized the outcome of 75.0 % of patients among those with favorable outcome (9 out of 12) and 90.9 % of those with unfavorable outcome (10 out of 11), demonstrating the high capacity of this analysis to predict the patients' outcome.

These results highlight the added prognostic value of dynamic features of brain activity that are not captured by static or structural imaging alone. Current clinical algorithms for outcome prediction at the early stage of brain injury rely heavily on a combination of demographic, clinical, and electrophysiological indicators, which are often imprecise or non-informative in borderline cases. By contrast, our dynamic connectivity-based metric—specifically the Weighted Entropy—provides a robust early indicator of 3-months neurological recovery. This is particularly relevant for patients in the so-called "gray zone," where decisions regarding continuation or withdrawal of life-sustaining therapy often rely on uncertain prognosis. The present approach may thus help refine clinical decision-making by offering an individualized, neurobiologically grounded marker of recovery potential.

Our results must be interpreted with caution and a number of limitations should be borne in mind. The first is related to the limited sample size that limits the generalizability of our finding. Despite representing one of the largest prospective fMRI cohorts of patients with acute DoC to date, we acknowledge that the present findings require validation in larger samples with stricter inclusion criteria to minimize potential confounding effects. In addition, the parameter space of our brain state analysis was not exhaustively explored, which may limit the generalizability of our findings. For example, in the present study we have chosen the window size (30 TRs) and step size (16 TRs) based on prior studies which have been shown to provide a good balance between temporal resolution and estimation reliability, we did not perform a formal sensitivity analysis to evaluate how alternative parameter choices might affect the structure of identified brain states or the performance of the prognostic model. Future studies could benefit from systematically exploring a broader parameter space or even implement other methods of connectivity estimation such as LEiDA (Deco et al., 2019) to further assess the robustness and generalizability of the findings. Another limitation of this study is the use of Pearson correlation to estimate functional connectivity, which captures only linear relationships between regions; future work should explore non-linear connectivity measures, such as mutual information or phase synchronization, to better capture the complex and potentially nonlinear dynamics of brain networks in patients with DoC. Another limitation is that we did not apply graph-theoretical measures to characterize the topological properties of the dynamic connectivity patterns. While such approaches have proven valuable for quantifying network integration, segregation, and hub structure, our analysis focused on state-wise connectivity and entropy measures. Future studies could benefit from incorporating graph-based metrics to gain deeper insights into the organizational principles underlying brain dynamics in disorders of consciousness.

While the present study focused on a predefined set of cortical regions, particularly subdivisions of the default mode (DMN), we acknowledge that this targeted approach may overlook the broader contributions of other brain structures. Consciousness arises from the dynamic interplay between cortical and subcortical systems, including arousal-related nuclei such as the brainstem, thalamus, and basal forebrain (Edlow et al., 2020), which were not directly addressed in our current analysis. Our choice to concentrate on the DMN and its midline components—such as the posterior cingulate cortex and medial prefrontal cortex—was guided by the anterior forebrain mesocircuit framework and grounded in prior evidence indicating the prognostic relevance of DMN connectivity in disorders of consciousness (Malagurski et al., 2019; Peran et al., 2020). These regions have consistently emerged as key hubs whose preservation or recovery is associated with improved neurological outcomes.

However, the use of whole-brain analytical models could offer a more comprehensive understanding of the spatial and temporal scales of dysfunction and recovery following severe brain injury. Such approaches may reveal additional, and potentially synergistic, mechanisms of impairment or compensation involving subcortical and arousal-related systems. Additionally, due to the limited sample size, we were not able to perform a reliable dissociation between different etiologies of brain injury, such as traumatic versus anoxic causes. Although both groups were included in the study, the number of patients in each subgroup was insufficient to support statistically meaningful comparisons. Future studies with larger and more balanced cohorts will be necessary to determine whether specific injury mechanisms give rise to distinct dynamic connectivity profiles.

To further evaluate the generality of our findings, we conducted an exploratory whole-brain analysis using the complete Willard atlas. This analysis yielded qualitatively similar results to those obtained within the DMN, indicating that the overall pattern of reduced integration and entropy in acute DoC extends beyond default-mode regions. However, the substantially larger dimensionality of the full-brain connectivity space ($499 \times 499$) introduced important limitations. The increased number of possible configurations led to the emergence of sparsely populated or unstable clusters, reflecting insufficient sampling of the full state space with the available data (Fig. S5). Consequently, only the high- and low-entropy states (States 5 and 6) remained robust, while intermediate states became less reliable. These observations highlight both the scalability of the current approach and its sensitivity to data dimensionality, underscoring the need for larger datasets and longer acquisitions to achieve stable whole-brain dynamic characterizations in future work.

We have observed that acute DoC is related to a critical reorganization of functional connectivity, which was characterized by a critical shift toward less informative DMN anchored brain states. This result is in line with converging evidence suggesting that structural and metabolic integrity of DMN is necessary, though not solely sufficient, for consciousness recovery from severe brain injury. Together, our results suggest that, during acute DoC, coordinated brain activity is largely restricted to a rigid functional configuration characterized by lower entropy and weaker long-distance correlations within the fronto-parietal mesocircuit. We suggest that our results allow for early and accurate neuroprognostication and hold promise of becoming a valuable new tool to assist decision-making in this challenging setting. Finally, it can be argued that the real-time detection of this pattern and its reinforcement through pharmacological or externally induced manipulations could represent a promising avenue for the therapeutic of consciousness.

## Study funding

This work was supported by the 'Association des Traumatisés du Crâne et de la Face', 'Fondation de l'Avenir', and Grant funding from University Hospital of Toulouse. Sponsors had no role in study design, data collection, data analysis, data interpretation or writing of the report

## Code and data availability

All data was processed using custom MATLAB and Python scripts. Codes are available at https://github.com/dellabellagabriel/coma3d. Data used in this paper will be available upon reasonable request (EBRAINS).

## CRediT authorship contribution statement

**Gabriel Della Bella:** Writing – original draft, Software, Formal analysis, Data curation. **Benjamine Sarton:** Writing – original draft, Supervision, Investigation, Data curation. **Giulia Maria Mattia:** Writing – original draft, Methodology, Data curation. **Patrice Peran:** Resources, Methodology. **Walter Lamberti:** Methodology, Formal analysis,

Conceptualization. **Pablo Barttfeld:** Writing – review & editing, Writing – original draft, Validation, Supervision, Software, Methodology, Investigation, Formal analysis, Conceptualization. **Stein Silva:** Writing – review & editing, Writing – original draft, Visualization, Validation, Supervision, Resources, Project administration, Methodology, Funding acquisition, Formal analysis, Conceptualization.

## Declaration of competing interest

The authors declare that they have no known competing financial interests or personal relationships that could have appeared to influence the work reported in this paper.

## Acknowledgements

The authors thank the technicians and engineers of the Neuroimaging Platform from ToNIC laboratory, the "Centre Investigation Clinique" CIC 1436, and the medical and nurse staff of the Critical Care Units of the University Hospital of Toulouse for their active participation in the neuroimaging studies in acute DoC patients. STIC AMSUD provided financial support which allowed this CONICET / INSERM collaboration.

## Supplementary materials

Supplementary material associated with this article can be found, in the online version, at doi:10.1016/j.neuroimage.2025.121657.

## References

Ahmadi, S., Sarveazad, A., Babahajian, A., Ahmadzadeh, K., Yousefifard, M., 2023. Comparison of Glasgow Coma Scale and Full Outline of UnResponsiveness score for prediction of in-hospital mortality in traumatic brain injury patients: a systematic review and meta-analysis. Eur. J. Trauma Emerg. Surg. agosto de 49 (4), 1693–1706.

Allen, E.A., Damaraju, E., Plis, S.M., Erhardt, E.B., Eichele, T., Calhoun, V.D., 2014. Tracking whole-brain connectivity dynamics in the resting State. Cereb Cortex N Y NY. marzo de 24 (3), 663–676.

Andrews-Hanna, J.R., Reidler, J.S., Sepulcre, J., Poulin, R., Buckner, R.L., 2010. Functional-anatomic fractionation of the brain's default network. Neuron. de febrero de 65 (4), 550–562.

Baars, B.J., 2005. Global workspace theory of consciousness: toward a cognitive neuroscience of human experience. En Progress Brain Res. 45–53 [Internet]. Elsevier [citado 14 de marzo de 2022]Disponible en. https://linkinghub.elsevier.com/retrieve/pii/S0079612305500049.

Barttfeld, P., Uhrig, L., Sitt, J.D., Sigman, M., Jarraya, B., Dehaene, S., 2015. Signature of consciousness in the dynamics of resting-state brain activity. Proc. Natl. Acad. Sci. 20 de enero de 112 (3), 887–892.

Boly, M., Balteau, E., Schnakers, C., Degueldre, C., Moonen, G., Luxen, A., et al., 2007. Baseline brain activity fluctuations predict somatosensory perception in humans. Proc. Natl. Acad. Sci. de julio de 104 (29), 12187–12192.

Boly, M., Massimini, M., Garrido, M.I., Gosseries, O., Noirhomme, Q., Laureys, S., et al., 2012. Brain connectivity in disorders of consciousness. Brain Connect 2 (1), 1–10.

Carhart-Harris, R., Leech, R., Hellyer, P., Shanahan, M., Feilding, A., Tagliazucchi, E., et al., 2014. The entropic brain: a theory of conscious states informed by neuroimaging research with psychedelic drugs. Front. Hum. Neurosci. [Internet] [citado 10 de agosto de 2022];8. Disponible en https://www.frontiersin.org/articles/10.3389/fnhum.2014.00020.

Deco, G., Cruzat, J., Cabral, J., Tagliazucchi, E., Laufs, H., Logothetis, N.K., et al., 2019. Awakening: predicting external stimulation to force transitions between different brain states. Proc. Natl. Acad. Sci. 116 (36), 18088–18097, 3 de septiembre de.

Dehaene, S., Changeux, J.P., 2011. Experimental and theoretical approaches to conscious processing. Neuron. abril de 70 (2), 200–227.

Demertzi, A., Antonopoulos, G., Heine, L., Voss, H.U., Crone, J.S., de, L., Angeles, C., et al., 2015. Intrinsic functional connectivity differentiates minimally conscious from unresponsive patients. Brain. septiembre de 138 (9), 2619–2631.

Demertzi, A., Tagliazucchi, E., Dehaene, S., Deco, G., Barttfeld, P., Raimondo, F., et al., 2019. Human consciousness is supported by dynamic complex patterns of brain signal coordination. Sci. Adv. febrero de 5 (2), eaat7603.

Edlow, B.L., Barra, M.E., Zhou, D.W., Foulkes, A.S., Snider, S.B., Threlkeld, Z.D., et al., 2020. Personalized connectome mapping to guide targeted therapy and promote recovery of consciousness in the intensive care unit. Neurocri.t Care. octubre de 33 (2), 364–375.

Edlow, B.L., Claassen, J., Schiff, N.D., Greer, D.M., 2021. Recovery from disorders of consciousness: mechanisms, prognosis and emerging therapies. Nat. Rev. Neurol. 17 (3), 135–156.

Fridman, E.A., Beattie, B.J., Broft, A., Laureys, S., Schiff, N.D., 2014. Regional cerebral metabolic patterns demonstrate the role of anterior forebrain mesocircuit dysfunction in the severely injured brain. Proc. Natl. Acad. Sci. de abril de 111 (17), 6473–6478.

Giacino, J.T., Fins, J.J., Laureys, S., Schiff, N.D., 2014. Disorders of consciousness after acquired brain injury: the state of the science. Nat. Rev. Neurol. febrero de 10 (2), 99–114.

Maas, A.I.R., Menon, D.K., Adelson, P.D., Andelic, N., Bell, M.J., Belli, A., et al., 2017. Traumatic brain injury: integrated approaches to improve prevention, clinical care, and research. Lancet Neurol. diciembre de 16 (12), 987–1048.

Malagurski, B., Péran, P., Sarton, B., Vinour, H., Naboulsi, E., Riu, B., et al., 2019. Topological disintegration of resting state functional connectomes in coma. NeuroImage. julio de 195, 354–361.

Mateos, D.M., Wennberg, R., PV, J.L., 2016. Statistical mechanics of consciousness: maximization of information content of network is associated with conscious awareness. Phys. Rev. E 94 (5–1), 052402.

Mateos, D.M., Guevara Erra, R., Wennberg, R., Perez Velazquez, J.L, 2018. Measures of entropy and complexity in altered states of consciousness. Cogn Neurodyn. febrero de 12 (1), 73–84.

Mattia, G.M., Sarton, B., Villain, E., Vinour, H., Ferre, F., Buffieres, W., et al., 2022. Multimodal MRI-based whole-brain assessment in patients In anoxoischemic coma by using 3D convolutional neural networks. Neurocrit. Care 37 (Suppl 2), 303–312.

Michel, C.M., Koenig, T., 2018. EEG microstates as a tool for studying the temporal dynamics of whole-brain neuronal networks: a review. NeuroImage. octubre de 180, 577–593.

Moseby-Knappe, M., Westhall, E., Backman, S., Mattsson-Carlgren, N., Dragancea, I., Lybeck, A., et al., 2020. Performance of a guideline-recommended algorithm for prognostication of poor neurological outcome after cardiac arrest. Intensive Care Med. octubre de 46 (10), 1852–1862.

Nolan, J.P., Sandroni, C., Böttiger, B.W., Cariou, A., Cronberg, T., Friberg, H., et al., 2021. European Resuscitation Council and European Society of Intensive Care Medicine guidelines 2021: post-resuscitation care. Intensive Care Med. abril de 47 (4), 369–421.

Peran, P., Malagurski, B., Nemmi, F., Sarton, B., Vinour, H., Ferre, F., et al., 2020. Functional and structural integrity of frontoparietal connectivity in traumatic and anoxic coma. Crit. Care Med. agosto de 48 (8), e639–e647.

Richiardi, J., Altmann, A., Milazzo, A.C., Chang, C., Chakravarty, M.M., Banaschewski, T., et al., 2015. Correlated gene expression supports synchronous activity in brain networks. Science. de junio de 348 (6240), 1241–1244.

Sandroni, C., Cronberg, T., Sekhon, M., 2021. Brain injury after cardiac arrest: pathophysiology, treatment, and prognosis. Intensive Care Med. diciembre de 47 (12), 1393–1414.

Sarton, B., Tauber, C., Fridman, E., Péran, P., Riu, B., Vinour, H., et al., 2024. Neuroimmune activation is associated with neurological outcome in anoxic and traumatic coma. Brain. 4 de abril de 147 (4), 1321–1330.

Schiff, N.D., 2024. Toward an interventional science of recovery after coma. Neuron. de mayo de 112 (10), 1595–1610.

Schnakers, C., Majerus, S., Giacino, J., Vanhaudenhuyse, A., Bruno, M.A., Boly, M., et al., 2008. A French validation study of the Coma Recovery Scale-revised (CRS-R). Brain Inj. enero de 22 (10), 786–792.

Silva, S., Alacoque, X., Fourcade, O., Samii, K., Marque, P., Woods, R., et al., 2010. Wakefulness and loss of awareness: brain and brainstem interaction in the vegetative state. Neurol. de enero de 74 (4), 313–320.

Silva, S., de Pasquale, F., Vuillaume, C., Riu, B., Loubinoux, I., Geeraerts, T., et al., 2015. Disruption of posteromedial large-scale neural communication predicts recovery from coma. Neurol. de diciembre de 85 (23), 2036–2044.

Storm, J.F., Klink, P.C., Aru, J., Senn, W., Goebel, R., Pigorini, A., et al., 2024. An integrative, multiscale view on neural theories of consciousness. Neuron. mayo de 112 (10), 1531–1552.

Uhrig, L., Sitt, J.D., Jacob, A., Tasserie, J., Barttfeld, P., Dupont, M., et al., 2018. Resting-state dynamics as a cortical signature of anesthesia in monkeys. Anesthesiology. 1 de noviembre de 129 (5), 942–958.

Vanhaudenhuyse, A., Noirhomme, Q., Tshibanda, L.J.F., Bruno, M.A., Boveroux, P., Schnakers, C., et al., 2010. Default network connectivity reflects the level of consciousness in non-communicative brain-damaged patients. Brain. enero de 133 (1), 161–171.

Wijdicks, E.F.M., Bamlet, W.R., Maramattom, B.V., Manno, E.M., McClelland, R.L., 2005. Validation of a new coma scale: the FOUR score. Ann. Neurol. octubre de 58 (4), 585–593.